O-GlcNAcylation regulates dopamine neuron function, survival and degeneration in Parkinson disease

Byeong Eun Lee,[1] Hye Yun Kim,[1] Hyun-Jin Kim,[1] Hyeongsun Jeong,[1] Byung-Gyu Kim,[2] Ha-Eun Lee,[1] Jieun Lee,[1] Han Byeol Kim,[3] Seung Eun Lee,[4] Yong Ryoul Yang,[5] Eugene C. Yi,[3] John A. Hanover,[6] Kyungjae Myung,[1,2] Pann-Ghill Suh,[1,7] Taejoon Kwon[1] and Jae-Ick Kim[1]

See Hart and Huang (doi:10.1093/brain/awaa398) for a scientific commentary on this article.

The dopamine system in the midbrain is essential for volitional movement, action selection, and reward-related learning. Despite its versatile roles, it contains only a small set of neurons in the brainstem. These dopamine neurons are especially susceptible to Parkinson's disease and prematurely degenerate in the course of disease progression, while the discovery of new therapeutic interventions has been disappointingly unsuccessful. Here, we show that O-GlcNAcylation, an essential post-translational modification in various types of cells, is critical for the physiological function and survival of dopamine neurons. Bidirectional modulation of O-GlcNAcylation importantly regulates dopamine neurons at the molecular, synaptic, cellular, and behavioural levels. Remarkably, genetic and pharmacological upregulation of O-GlcNAcylation mitigates neurodegeneration, synaptic impairments, and motor deficits in an animal model of Parkinson's disease. These findings provide insights into the functional importance of O-GlcNAcylation in the dopamine system, which may be utilized to protect dopamine neurons against Parkinson's disease pathology.

1 School of Life Sciences, Ulsan National Institute of Science and Technology (UNIST), Ulsan 44919, Republic of Korea
2 Center for Genomic Integrity, Institute for Basic Science (IBS), Ulsan 44919, Republic of Korea
3 Department of Molecular Medicine and Biopharmaceutical Sciences, Graduate School of Convergence Science and Technology, College of Medicine and College of Pharmacy, Seoul National University, Seoul 03080, Republic of Korea
4 Research Animal Resource Center, Korea Institute of Science and Technology (KIST), Seoul 02792, Republic of Korea
5 Aging Research Center, Korea Research Institute of Bioscience and Biotechnology (KRIBB), Daejeon 34141, Republic of Korea
6 Laboratory of Cell and Molecular Biology, National Institute of Diabetes and Digestive and Kidney (NIDDK), National Institute of Health (NIH), Bethesda, Maryland, USA
7 Korea Brain Research Institute (KBRI), Daegu 41062, Republic of Korea

Correspondence to: Jae-Ick Kim, PhD
School of Life Sciences, Building 110, Room 601-5, Ulsan National Institute of Science and Technology (UNIST)
Ulsan 44919, Republic of Korea
E-mail: jikim220@unist.ac.kr

Introduction

The midbrain dopamine system comprises a group of dopamine-releasing neurons and their axonal projections in the brain (Gerfen and Surmeier, 2011). Although the dopamine system contains only a small set of neurons, this little population exerts a strong influence over a large area of the brain through dense and wide axonal arborizations (Matsuda *et al.*, 2009). Dopamine neurons orchestrate a variety of neural functions, including voluntary movement, action selection, motivation, reward-related learning and memory (Schultz, 2007; Berke, 2018). In Parkinson's disease, however, dopamine neurons in substantia nigra pars compacta (SNc) are selectively vulnerable owing to their molecular and physiological features and they prematurely degenerate in the progression of the disease (Brichta and Greengard, 2014; Roselli and Caroni, 2015). Unfortunately, the therapeutic arsenal for the treatment of Parkinson's disease have long remained limited to a group of dopamine-related drugs and deep brain stimulation, which provide only a temporary relief of the major symptoms in Parkinson's disease. Therefore, continuing efforts to search for alternative and better therapeutic strategies are necessarily needed.

O-GlcNAcylation is a post-translational modification (PTM), in which a single O-linked β-*N*-acetylglucosamine (*O*-GlcNAc) is attached to serine and/or threonine residues in various nuclear, cytosolic, and mitochondrial proteins (Holt and Hart, 1986; Love *et al.*, 2003). This modification is evolutionarily well conserved from bacteria to mammals including humans and it has been shown that *O*-GlcNAcylation regulates key cellular processes, such as transcription, translation, signal transduction, and protein homeostasis (Hart *et al.*, 2011; Akan *et al.*, 2018). Attachment of *O*-GlcNAc to target proteins is dynamic, reversible, and *O*-GlcNAcylation can interact with other PTMs, including phosphorylation (Wang *et al.*, 2008, 2010*b*; Yang and Qian, 2017). Notably, *O*-GlcNAc modification is highly abundant in the mammalian brain and many neuron-specific proteins undergo *O*-GlcNAcylation (Cole and Hart, 2001; Akimoto *et al.*, 2003; Khidekel *et al.*, 2004; Vosseller *et al.*, 2006), while our understanding of the physiological role of *O*-GlcNAcylation remains rudimentary in the brain. Emerging evidence has demonstrated the role of *O*-GlcNAcylation in the regulation of energy metabolism and feeding behaviour (Ruan *et al.*, 2014; Lagerlof *et al.*, 2016; Dai *et al.*, 2018). Interestingly, *O*-GlcNAc modification appears to decline during both normal and pathological ageing, as in Alzheimer's disease (Rex-Mathes *et al.*, 2001; Deng *et al.*, 2009; Liu *et al.*, 2012). Furthermore, the upregulation of neuronal *O*-GlcNAcylation could improve cognitive function in the aged mice (Wheatley *et al.*, 2019) and pharmacological elevation of *O*-GlcNAc level may rescue memory impairment in Alzheimer's disease mouse model, possibly via attenuating protein aggregation (Yuzwa *et al.*, 2012; Kim *et al.*, 2013). Importantly, α-synuclein, a presynaptic protein that is enriched in dopamine and other neurons, is pathologically linked to Parkinson's disease and also *O*-GlcNAcylated. Since *O*-GlcNAcylation is remarkably ubiquitous in the brain, *O*-GlcNAc modification in dopamine neurons could be essential for coordinating various neuronal functions and represent a potential target for therapeutic intervention that can help alleviate the symptoms of Parkinson's disease.

In this study, we investigated whether *O*-GlcNAcylation plays a pivotal role in dopamine neurons and whether the manipulation of *O*-GlcNAcylation can protect dopamine neurons from the pathology of Parkinson's disease. First, by downregulating the *O*-GlcNAc modification in dopamine neurons, we found that *O*-GlcNAcylation is indispensable for the survival and maintenance of the midbrain dopamine system. Reduced *O*-GlcNAc level caused the dysfunction and degeneration of dopamine neurons, which eventually led to premature animal death. On the contrary, upregulation of *O*-GlcNAcylation did not produce any adverse effects on dopamine neurons, but facilitated synaptic functions at dopamine synapses. At the behavioural level, downregulation of *O*-GlcNAcylation caused severe motor deficits, while upregulated *O*-GlcNAcylation did not negatively affect any motor and cognitive functions. Most excitingly, elevated *O*-GlcNAcylation in dopamine neurons was protective against α-synuclein-induced Parkinson's disease pathology, making dopamine neurons intact and physiologically functional. Together, our data demonstrate that *O*-GlcNAcylation is vital for the survival, maintenance, and physiological functions of dopamine neurons. Moreover, upregulating *O*-GlcNAc modification can alleviate the degeneration, functional impairments, and motor deficits induced in a Parkinson's disease animal model.

Materials and methods

Animals

Young (3 weeks old, male and female) and adult (8–20 weeks old, male and female) mice were used for this study. All experimental procedures were conducted in accordance with protocols approved by Institutional Animal Care and Utilization Committee of UNIST. More detailed information is provided in the Supplementary material.

Immunohistochemistry

For immunofluorescence staining, mice were anaesthetized by intraperitoneal injection of zoletil and rompun mixture solution and perfused transcardially with phosphate buffer, followed by 4% paraformaldehyde. Brains were rapidly removed and maintained in 4% paraformaldehyde (PFA) at 4°C for overnight. Fixed brains were transferred to 30% sucrose in 0.01 M phosphate buffer for cryoprotection. Obtained brain sections were washed with phosphate-buffered saline (PBS), PBST and blocked with PBST containing 10% normal goat serum and 2% bovine serum albumin. After blocking, brain sections were incubated sequentially with primary and secondary antibodies. More detailed information is provided in the Supplementary material.

Biocytin labelling and immunostaining of biocytin-filled neurons

For examining the morphology, dendritic arborization, and the number of dendritic spines in a single dopamine neuron, potassium-based internal solution with 0.2% biocytin was loaded to dopamine neurons in SNc and ventral tegmental area (VTA) for 30 min. More detailed information is provided in the Supplementary material.

Brain slice preparation for electrophysiology

Coronal brain slices containing dorsolateral striatum-nucleus accumbens core (DLS-NAc) or SNc-VTA were obtained for whole-cell patch clamp recording and fast-scanning cyclic voltammetry (FSCV). More detailed information is provided in the Supplementary material.

Electrophysiology, optogenetic stimulation and pharmacology

Dopamine neurons and spiny projection neurons were visually identified by conventional IR-DIC optics. Whole-cell voltage clamp recordings were made with borosilicate glass pipettes filled with Cs^+-based low Cl^- internal solution. More detailed information is provided in the Supplementary material.

Fast-scanning cyclic voltammetry

Extracellular dopamine release was recorded by FSCV using carbon-fibre microelectrodes at the DLS and NAc. More detailed information is provided in the Supplementary material.

Precipitation of *O*-GlcNAcylated proteins by succinylated wheat germ agglutinin and mass spectrometry

Mice were anaesthetized with isoflurane and euthanized by decapitation. The brains were rapidly removed and cut in a Vibratome in cold artificial CSF solution. The striatum and midbrain dopamine regions were separately dissected and frozen in liquid nitrogen and then stored at −80°C in a deep freezer. More detailed information is provided in the Supplementary material.

Proteomic analysis of *O*-GlcNAc-modified proteins

We searched the MS/MS proteomics data against a mouse UniProt reference proteome database (Version 2019_10) using the MaxQuant platform (Version 1.5.8.3). Trypsin/P was specified as the cleavage enzyme, allowing up to two missed cleavages. More detailed information is provided in the Supplementary material.

Virus generation

We used pHM6-α-synuclein-A53T (Addgene #40825) construct to generate AAV-α-synuclein-A53T and AAV-α-synuclein-A53T-mediated mouse model of Parkinson's disease. More detailed information is provided in the Supplementary material.

Stereotaxic viral injection

Stereotaxic virus injections were conducted on male and female mice over 8 weeks old [dopamine transporter (DAT)-Cre;$Oga^{+/+}$, DAT-Cre;$Oga^{fl/fl}$, DAT-Cre;Ai32;$Oga^{+/+}$, DAT-Cre;Ai32;$Oga^{fl/fl}$, DAT-Cre] and performed using a stereotaxic system. More detailed information is provided in the Supplementary material.

Pharmacological *O*-GlcNAcase inhibition in Parkinson's disease mouse model

We injected Thiamet G daily for 2 weeks by intraperitoneal injection. Vehicle (10% DMSO in saline) was injected in control DAT-Cre mice. More detailed information is provided in the Supplementary material.

Behavioural tests

Behavioural experiments were conducted during the day (10 am to 4 pm) under dim light conditions except for the accelerating rotarod, elevated plus maze, pole test, grip strength test, and tail suspension test. More detailed information is provided in the Supplementary material.

Statistics

All data were analysed using Clampfit 10.7 (Molecular Devices), Mini Analysis (Synaptosoft), OriginPro 2017 (OriginLab), and ImageJ (NIH). Measured values and the details of statistical analysis were presented in the figure legends and Supplementary Table 1. More detailed information is provided in the Supplementary material.

Data availability

All data are available from the corresponding author upon request.

Results

O-GlcNAcylation is crucial for the survival and maintenance of dopamine neurons

Unlike phosphorylation, *O*-GlcNAcylation is solely mediated by a pair of enzymes in the mammalian tissues. Transferring of *O*-GlcNAc is carried out by *O*-GlcNAc transferase (OGT), whereas *O*-GlcNAcase (OGA) functions to remove *O*-GlcNAc from target proteins (Yang and Qian, 2017).

Both enzymes are also predominantly expressed in the brain (Zachara and Hart, 2006; Akan *et al.*, 2018). To investigate the functional importance of *O*-GlcNAcylation in dopamine neurons, we first sought to determine whether the downregulation of *O*-GlcNAcylation affects the midbrain dopamine neurons. We created a conditional knockout (cKO) mouse line where the level of *O*-GlcNAcylation was downregulated selectively in dopamine neurons by utilizing DAT-IRES-Cre mice (in which Cre recombinase is selectively expressed in DAT-expressing neurons). We crossed DAT-IRES-Cre mice with *Ogt* floxed (*Ogt*$^{fl/fl}$) mice to produce DAT-Cre;*Ogt*$^{fl/fl}$ mice (Fig. 1A). DAT-Cre;*Ogt*$^{fl/fl}$ mice displayed normal body weight during the first three postnatal weeks, but they started to grow slowly and stopped gaining more body weight from 5 weeks of age. When DAT-Cre;*Ogt*$^{fl/fl}$ mice matured to adulthood, their mean body weight was significantly lower than the wild-type littermates (DAT-Cre;*Ogt*$^{+/+}$) (Fig. 1B). Notably, DAT-Cre;*Ogt*$^{fl/fl}$ mice also exhibited premature death at around 8 to 15 weeks of age (Fig. 1C).

We asked whether the downregulation of *O*-GlcNAcylation exerts detrimental effects on dopamine neurons, possibly underlying growth defect and early death. To this end, we investigated dopamine neuron abnormalities in mature DAT-Cre;*Ogt*$^{fl/fl}$ mice by double immunostaining for tyrosine hydroxylase (TH) and *O*-GlcNAc. We could first confirm that the level of *O*-GlcNAcylation was considerably diminished in the cell bodies of both the SNc and VTA (Fig. 1G). We next found substantial loss and deficits of midbrain dopamine neurons in the SNc and VTA (Fig. 1D–F). The number, TH-positive area, and TH intensity of dopamine neurons were dramatically reduced in both areas (Fig. 1H–J). Notably, the size of a single cell body was also markedly decreased in dopamine neurons by the downregulation of *O*-GlcNAcylation (Fig. 1K). Meanwhile, dopamine neurons form exceptionally dense axonal arborization in the striatum (Matsuda *et al.*, 2009). Significant loss of both TH and DAT immunoreactivities was observed from dopaminergic axons in the DLS and NAc, the major target areas of midbrain dopamine neurons (Fig. 1L–S), indicating that the downregulation of *O*-GlcNAcylation leads to massive loss of axons and synapses in dopamine neurons. We then examined structural abnormalities in 3-week-old DAT-Cre;*Ogt*$^{fl/fl}$ mice. We found that, although the extent of defects in dopamine neurons was less than mature mice, 3-week-old DAT-Cre;*Ogt*$^{fl/fl}$ mice also exhibited a severe loss of axons in the striatum (Supplementary Fig. 1). Considering postmitotic expression of DAT in dopamine neurons, these data suggest that downregulation of *O*-GlcNAcylation in dopamine neurons leads to early loss of axonal arborizations and synapses followed by neuronal degeneration and premature animal death.

Downregulation of O-GlcNAcylation in dopamine neurons causes functional impairments at dopamine synapses

Given the importance of *O*-GlcNAc modification in key cellular processes, downregulation in *O*-GlcNAcylation can affect physiological properties of dopamine neurons. To examine functional consequences caused by the downregulation of *O*-GlcNAcylation in dopamine neurons, we performed FSCV to monitor the release of dopamine at dopamine synapses. As explained above, a single dopamine neuron forms dense and widely spread axonal arborization in multiple brain areas, especially the dorsal and ventral striatum (Matsuda *et al.*, 2009). We expressed channelrhodopsin 2 (ChR2) in dopamine neurons by crossing DAT-Cre;*Ogt*$^{+/+}$ and DAT-Cre;*Ogt*$^{fl/fl}$ mice with transgenic mice containing a conditional floxed allele of ChR2 in the Rosa26 locus (Ai32 mice). Optogenetic stimulation of dopamine axons with brief light pulses evoked dopamine release from brain slices containing DLS and NAc in DAT-Cre;Ai32;*Ogt*$^{+/+}$ mice (Fig. 2A). Dopamine release, however, was completely abolished in the DLS of DAT-Cre;Ai32;*Ogt*$^{fl/fl}$ mice (Fig. 2B–D). In addition, a similar decrease in dopamine release was observed in the NAc (Fig. 2E and F), implicating that the attenuation of dopamine release is universal across the brain regions. New studies have revealed that dopamine neurons can co-transmit multiple neurotransmitters, including glutamate and γ-amminobutyric acid (GABA), in the striatum (Tritsch *et al.*, 2012; Kim *et al.*, 2015). We also checked the release of two neurotransmitters from dopamine synapses and found that co-transmission of glutamate and GABA, recorded in spiny projection neurons by optogenetically induced excitatory postsynaptic current (oEPSC) and inhibitory postsynaptic current (oIPSC), was severely impaired by the downregulation of *O*-GlcNAc in dopamine neurons (Fig. 2G and H). These data establish that *O*-GlcNAcylation is necessary for the normal synaptic functions of dopamine neurons and multiple neurotransmitters release at dopamine synapses are completely compromised by the loss of *O*-GlcNAcylation in dopamine neurons.

Upregulation of O-GlcNAcylation in dopamine neurons does not negatively affect neuronal structures

In the mammalian brain, removal of *O*-GlcNAc from proteins is mediated by a single enzyme, OGA. To test whether the upregulation of *O*-GlcNAcylation can have differential and opposite effects, we selectively deleted *Oga* in dopamine neurons. *Oga* floxed (*Oga*$^{fl/fl}$) mice were bred with DAT-IRES-Cre mice to generate DAT-Cre;*Oga*$^{fl/fl}$ mice (Fig. 3A). In previous findings, whole-body *Oga* KO mice died around birth (Yang *et al.*, 2012; Keembiyehetty *et al.*, 2015) and pan-neuronal knockout of *Oga* also caused
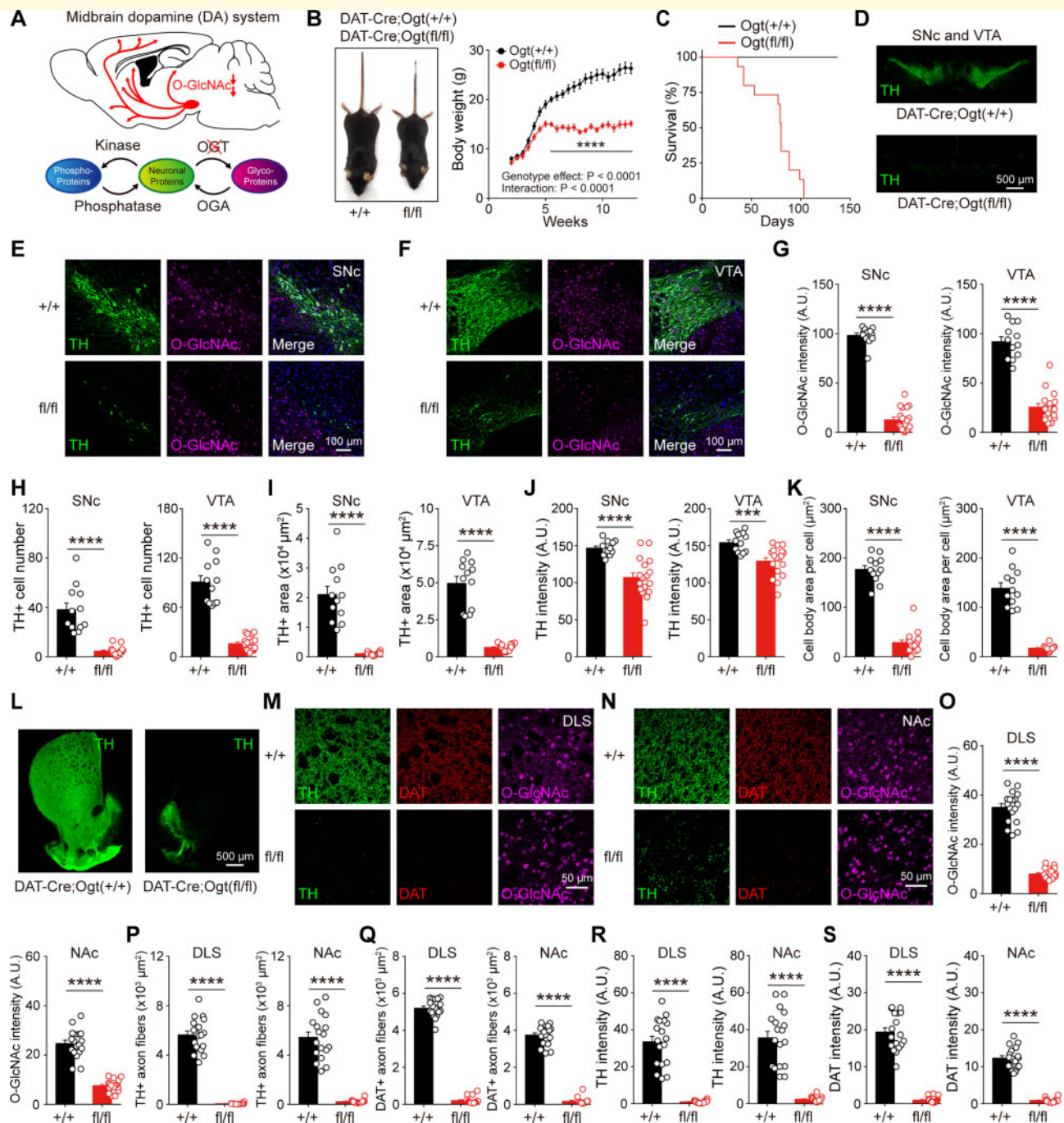
Figure 1 *O*-GlcNAcylation is crucial for the survival and maintenance of dopamine neurons. (**A**) Schematic illustration depicting selective downregulation of *O*-GlcNAc in dopamine neurons. (**B**) Body size and weight in DAT-Cre;*Ogt*^{+/+} and DAT-Cre;*Ogt*^{fl/fl} mice. (**C**) Survival rate of DAT-Cre;*Ogt*^{+/+} and DAT-Cre;*Ogt*^{fl/fl} mice. (**D**) TH + dopamine neurons in the midbrain. (**E** and **F**) Confocal images of TH and *O*-GlcNAc immunofluorescence in the midbrain of adult DAT-Cre;*Ogt*^{+/+} and DAT-Cre;*Ogt*^{fl/fl} mice. (**G–K**) Summary statistics for *O*-GlcNAc intensity, TH + cell number, TH + area, TH intensity, and individual cell body area. (**L**) Representative images of striatum and TH + dopamine axon fibres. (**M** and **N**) Confocal images of TH, DAT, and *O*-GlcNAc immunofluorescence in DLS and NAc. (**O–S**) Summary statistics for *O*-GlcNAc intensity, TH + axon fibres, DAT + axon fibres, TH intensity, and DAT intensity. Data were analysed by ordinary two-way ANOVA (**B**), log-rank test (**C**), and unpaired *t*-test (**G–K** and **O–S**). Data are represented as mean ± standard error of the mean (SEM). ***$P < 0.001$, ****$P < 0.0001$.
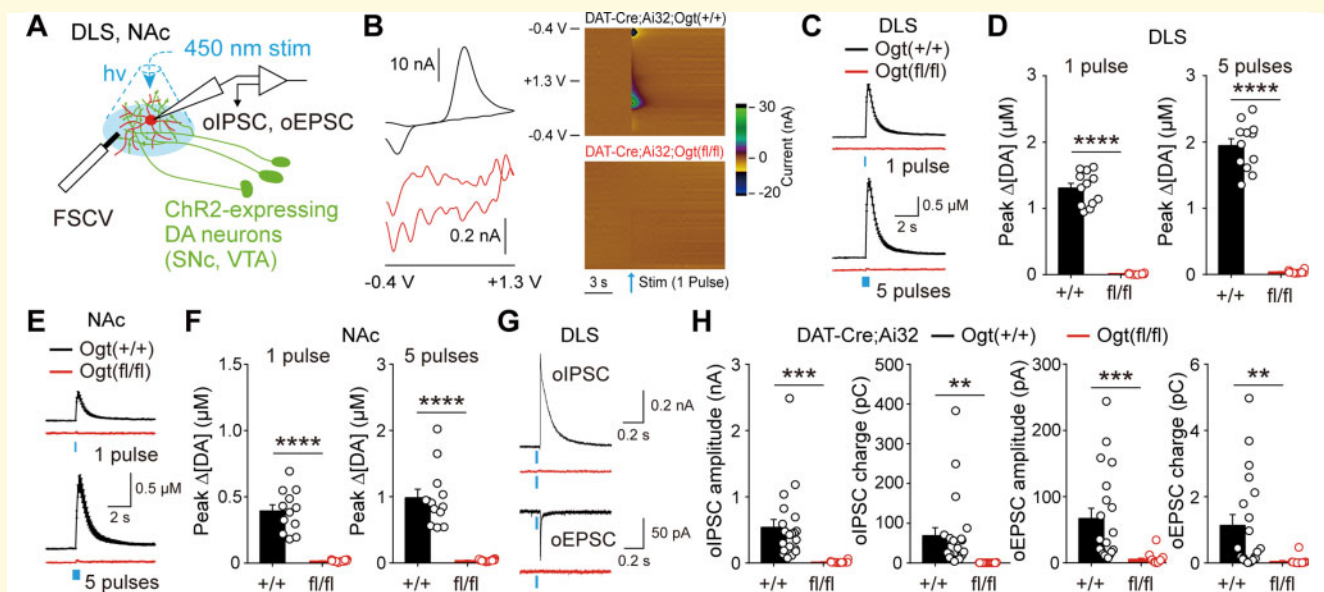
Figure 2 Downregulation of *O*-GlcNAcylation in dopamine neurons causes functional impairments at dopamine synapses. (A) Schematic illustration depicting electrophysiological recording of synaptic transmission at dopamine synapses. **(B)** 2D and colour-coded voltammograms showing oxidation and reduction peaks of dopamine release. **(C and D)** Summary statistics of dopamine release evoked by one pulse or five pulse stimulation in DLS. **(E and F)** Summary statistics of dopamine release evoked by one pulse or five pulse stimulation in NAc. **(G)** Representative recording traces for GABA and glutamate co-transmission at dopamine synapses. **(H)** Quantification of neurotransmitter co-transmission at dopamine synapses. Blue bar indicates optogenetic light stimulation. Data were analysed by unpaired *t*-test (**D**, **F** and **H**). Data are represented as mean ± SEM. *******P* < 0.01, ***P < 0.001, ****P < 0.0001.

early-onset obesity, growth defects, and metabolic dysregulation (Olivier-Van Stichelen *et al.*, 2017). Unlike DAT-Cre;*Ogt*^fl/fl^ mice, DAT-Cre;*Oga*^fl/fl^ mice survived to adulthood, and showed no obvious deleterious health effects. Although juvenile DAT-Cre;*Oga*^fl/fl^ mice temporarily gained more body weight, they were indistinguishable from wild-type littermates at adulthood (Fig. 3B). Overall, no structural abnormalities were found in midbrain dopamine neurons by the upregulation of *O*-GlcNAcylation. In SNc and VTA, it was apparent that the level of *O*-GlcNAcylation was considerably elevated in the cell bodies of both areas by the genetic deletion of *Oga* in dopamine neurons (Fig. 3D, E and Supplementary Fig. 2A and B). The number of TH-positive neurons, their area, and TH intensity were comparable between DAT-Cre;*Oga*^+/+^ and DAT-Cre;*Oga*^fl/fl^ mice (Fig. 3C–E and Supplementary Fig. 2A and B). We then checked potential morphological alterations of a single dopamine neuron by examining the patterns of dendritic arborization (Luo *et al.*, 2016). Increased *O*-GlcNAcylation did not affect dendritic branching (Fig. 3F–I) and spine densities (Fig. 3J and K) in dopamine neurons. In dopamine terminals, there were no pronounced changes in the intensities (TH, DAT) as well as the area of axonal fibres in DLS and NAc by *O*-GlcNAc elevation (Fig. 3L–N and Supplementary Fig. 2C and D). Thus, our data suggest that selective upregulation of *O*-GlcNAc modification in dopamine neurons does not negatively influence dopamine neuronal structures.

Elevated *O*-GlcNAcylation in dopamine neurons facilitates synaptic transmission at dopamine synapses

Upregulation of *O*-GlcNAcylation can influence key neuronal properties in the brain (Hwang and Rhim, 2019). Dopamine neurons spontaneously fire at a low rate, a mode called 'tonic firing'. Analysis of this tonic firing revealed that action potential characteristics were not changed by *O*-GlcNAc upregulation in SNc and VTA (Supplementary Fig. 3A–D). Additional determinants of intrinsic properties, such as input resistance and membrane excitability, also appeared not to be affected (Supplementary Fig. 3E–H). Hyperpolarization-activated cation current (Ih) and voltage sag are fundamental characteristics of dopamine neurons, which are vital for regulating neuronal properties and AP firing. In DAT-Cre;*Oga*^fl/fl^ mice, both Ih current and voltage sag in SNc dopamine neurons were comparable to those observed in wild-type littermates, while both of properties in VTA were only marginally affected by elevated *O*-GlcNAcylation (Supplementary Fig. 3I–P). Collectively, these observations indicate that increased *O*-GlcNAc modification does not lead to alterations in key intrinsic properties of midbrain dopamine neurons.

Dopamine neurons in SNc and VTA receive direct excitatory and inhibitory synaptic inputs from numerous brain areas (Watabe-Uchida *et al.*, 2012). We investigated whether
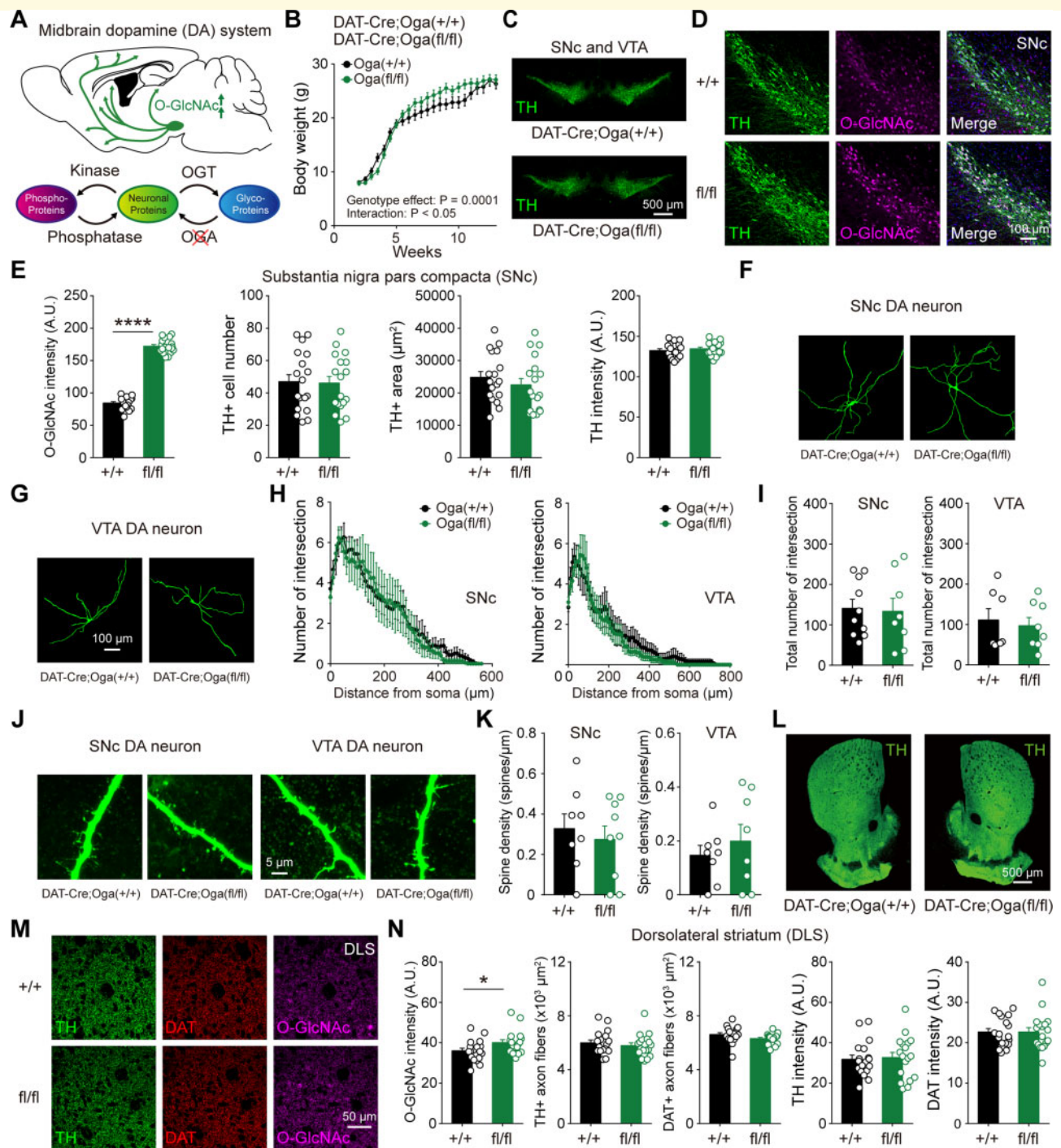
Figure 3 Upregulation of *O*-GlcNAcylation in dopamine neurons does not negatively affect neuronal structures. (**A**) Schematic illustration depicting selective upregulation of *O*-GlcNAc in dopamine neurons. (**B**) Body size and weight in DAT-Cre;*Oga*^{+/+} and DAT-Cre;*Oga*^{fl/fl} mice. (**C**) Midbrain TH + dopaminergic neurons in adult DAT-Cre;*Oga*^{+/+} and DAT-Cre;*Oga*^{fl/fl} mice. (**D**) Confocal images of TH and *O*-GlcNAc immunofluorescence in SNc. (**E**) Summary statistics of TH and *O*-GlcNAc immunoreactivities. (**F** and **G**) Representative confocal images of a single dopamine neuron in SNc and VTA by intracellular biocytin labelling. (**H**) Sholl analysis for the number of dendrite intersections in SNc and VTA dopamine neurons. (**I**) Total number of intersections in SNc and VTA dopamine neurons. (**J**) Representative confocal images of dendrite and dendritic spines in SNc and VTA dopamine neurons. (**K**) Quantification of spine density from dopamine neurons. (**L**) Low magnification images of striatum showing TH + dopamine axons in adult DAT-Cre;*Oga*^{+/+} and DAT-Cre;*Oga*^{fl/fl} mice. (**M**) Confocal images of TH, DAT, and *O*-GlcNAc immunofluorescence in DLS. (**N**) Summary statistics of *O*-GlcNAc, TH, and DAT immunoreactivities in axon fibres of DLS. Data were analysed by ordinary two-way ANOVA (**B**), unpaired *t*-test (**E**, **I**, **K** and **N**) and repeated measures two-way ANOVA (**H**). Data are represented as mean ± SEM. *$P < 0.05$, ****$P < 0.0001$.

synaptic transmission to midbrain dopamine neurons was changed by the upregulation of *O*-GlcNAcylation. We found that the amplitude of miniature excitatory postsynaptic current (mEPSC) was uniquely increased in SNc dopamine neurons of DAT-Cre;*Oga*^{fl/fl} mice, whereas other properties of mEPSC in midbrain dopamine neurons were not altered (Fig. 4A–D). Upregulated *O*-GlcNAcylation did not influence miniature inhibitory postsynaptic current (mIPSC) (Supplementary Fig. 4A–D). We then used OGA inhibitor (Thiamet G, 100 μM) and examined the acute effect of pharmacological upregulation of *O*-GlcNAcylation on mEPSC and mIPSC in midbrain dopamine neurons. Interestingly, the frequency of mIPSC in VTA was selectively increased by acute OGA inhibition, while mEPSCs were not changed in both SNc and VTA (Supplementary Fig. 4E–L), demonstrating that transient but non-specific elevation of *O*-GlcNAcylation in midbrain neural circuits can produce differential effects on spontaneous synaptic transmission to dopamine neurons.

If incoming excitatory synaptic transmission to dopamine neurons were potentiated, dopamine transmission in target brain regions of dopamine neurons would also be influenced by the upregulation of *O*-GlcNAcylation. To gauge how synaptic transmission is functionally affected at dopamine synapses, we generated DAT-Cre;Ai32;*Oga*^{fl/fl} mice by crossing DAT-Cre;*Oga*^{fl/fl} mice with Ai32 mice. We then utilized FSCV and examined the release of dopamine in DLS and NAc. Most notably, release of dopamine evoked by a single pulse or five pulses light stimulation mimicking phasic activation of dopamine neurons was significantly enhanced in DLS by increased *O*-GlcNAcylation (Fig. 4E and F). Although weaker, dopamine transmission was also enhanced in NAc (Fig. 4G and H), implying that the enhancement of
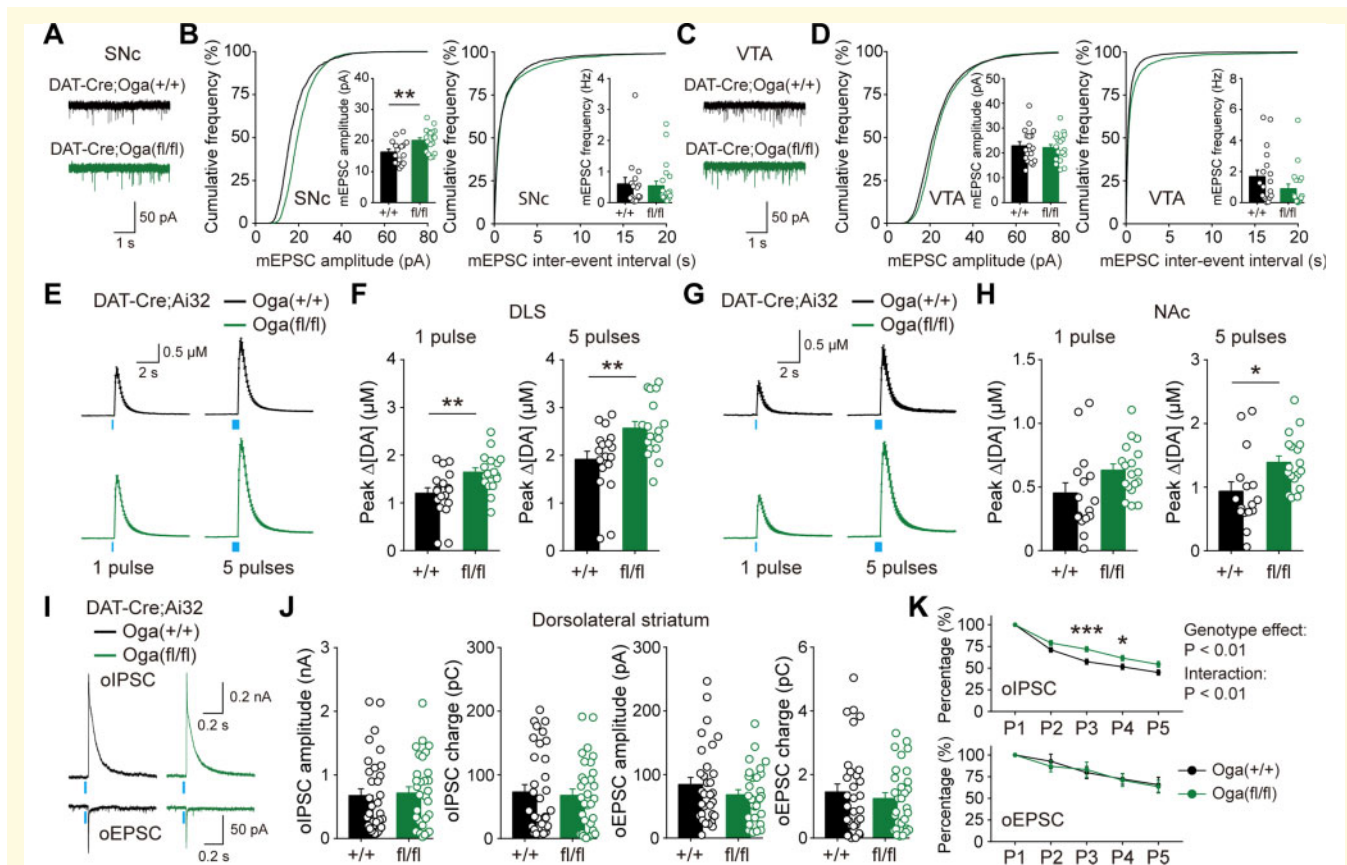

Figure 4 Elevated *O*-GlcNAcylation facilitates synaptic transmission at dopamine synapses. (A) Representative mEPSC recording traces in SNc. **(B)** Cumulative graph and summary statistics for mEPSC in SNc. **(C)** Representative mEPSC recording traces in VTA. **(D)** Cumulative graph and summary statistics for mEPSC in VTA. **(E and F)** Summary statistics of dopamine release evoked by one pulse or five pulse stimulation in DLS from DAT-Cre;Ai32;*Oga*^{+/+} and DAT-Cre;Ai32;*Oga*^{fl/fl} mice. **(G and H)** Summary statistics of dopamine release evoked by one pulse or five pulse stimulation in NAc. **(I)** Representative recording traces [optogenetically induced excitatory postsynaptic current (oEPSC) and inhibitory postsynaptic current (oIPSC)] made from spiny projection neurons (SPNs) in DLS. **(J)** Quantification of neurotransmitter co-transmission in DLS. **(K)** Attenuation of oIPSC and oEPSC by repetitive stimulations. Blue bar indicates optogenetic light stimulation. Data were analysed by unpaired *t*-test (**B**, **D**, **F**, **H** and **J**) and repeated measures two-way ANOVA followed by Sidak's *post hoc* test (**K**). Data are represented as mean ± SEM. *$P < 0.05$, **$P < 0.01$, ***$P < 0.001$.

dopamine release can universally occur at dopamine terminals across the brain by *O*-GlcNAc upregulation. On the other hand, upregulated *O*-GlcNAc did not promote GABA and glutamate co-transmission at dopamine synapses, which were recorded from spiny projection neurons in DLS (Fig. 4I and J). Interestingly, the attenuation of oIPSCs induced by consecutive optogenetic stimulations of dopamine terminals was slower in DAT-Cre;Ai32;*Oga*^fl/fl mice when compared with wild-type littermates (Fig. 4K). However, no difference was observed in the attenuation of oEPSC between the genotypes (Fig. 4K). Together, our data clearly show that selective upregulation of *O*-GlcNAcylation in dopamine neurons facilitates synaptic transmission at dopamine terminals, without altering intrinsic properties.

Manipulation of *O*-GlcNAcylation alters motor behaviours and the abundance of *O*-GlcNAcylated proteins

Very few studies have reported behavioural consequences of cell type-specific modulation of *O*-GlcNAcylation in the brain (Wang *et al.*, 2016). Given the versatile roles played by dopamine neurons in the brain, especially voluntary movement and motor learning, down- or upregulation of *O*-GlcNAcylation would affect neural functions at the level of animal behaviours. To probe the effect of *O*-GlcNAc downregulation in dopamine-mediated animal behaviours, we first evaluated locomotion in the open field test. Importantly, DAT-Cre;*Ogt*^fl/fl mice displayed severe hypoactivity and locomotive behaviour was remarkably diminished in the open field (Fig. 5A–C). In thigmotaxis, DAT-Cre;*Ogt*^fl/fl mice travelled less distance in exploring the peripheral zone of the open field than wild-type littermates (Fig. 5D). However, when the total time staying in each zone of the open field was compared, no difference was found between the genotypes (Supplementary Fig. 5A). Any changes in anxiety level were further assessed by elevated plus maze and DAT-Cre;*Ogt*^fl/fl mice did not largely show any signs of reduced anxiety (Supplementary Fig. 5B and C), demonstrating that anxiety was not altered by the downregulation of *O*-GlcNAc in dopamine neurons.

To gain a better insight into the nature of hypoactivity in DAT-Cre;*Ogt*^fl/fl mice, we next conducted the pole and rotarod tests. Time to descend in the pole test was significantly prolonged without any change in grip strength (Fig. 5E and Supplementary Fig. 5D) and performance in the rotarod test was considerably impaired in DAT-Cre;*Ogt*^fl/fl mice throughout the learning and test phases (Fig. 5F, G and Supplementary Fig. 5E). A significant increase in immobility time that reflects either a stress-coping strategy or behavioural despair was also observed in the tail suspension test in DAT-Cre;*Ogt*^fl/fl mice (Supplementary Fig. 5F). Among

many target areas, dopamine neurons project to the hippocampus as well and regulate hippocampus-dependent cognitive functions (Lisman and Grace, 2005). Lastly, we carried out contextual fear conditioning, which is dependent on the hippocampus and found that freezing was strikingly increased in DAT-Cre;*Ogt*^fl/fl mice (Supplementary Fig. 5G). Considering severe impairments in locomotion and motor learning, it is very likely that other behavioural deficits detected in DAT-Cre;*Ogt*^fl/fl mice may be more associated with defects in voluntary movement than cognitive impairments. With the above behavioural changes in mind, we now assessed the effects of enhanced *O*-GlcNAcylation on dopamine-modulated animal behaviours. Interestingly, functional changes in the dopamine neurons, including elevated dopamine release, did not lead to any obvious behavioural alterations in DAT-Cre;*Oga*^fl/fl mice, especially in locomotion and motor learning. DAT-Cre;*Oga*^fl/fl mice showed largely normal performance over a range of behavioural tests that we conducted (Fig. 5H–N and Supplementary Fig. 5H–N). Taken together, these data indicate that reduced *O*-GlcNAcylation in dopamine neurons disrupts motor behaviours, whereas upregulated *O*-GlcNAc does not negatively impact on dopamine-modulated behaviours.

As documented in earlier proteomics studies, a large number of neuronal proteins from mouse and human brains are modified by *O*-GlcNAcylation (Wani *et al.*, 2017). We sought to determine the candidate targets of *O*-GlcNAc modification in the midbrain dopamine region and its main target area, the striatum. *O*-GlcNAcylation in these regions may possibly underlie the effects of *O*-GlcNAc manipulation that we found in dopamine neurons. To achieve this, we dissected the midbrain dopamine area and striatum separately from wild-type and DAT-Cre;*Oga*^fl/fl mice. Then, we enriched *O*-GlcNAc-modified proteins from these brain samples and performed a shotgun proteomics experiment to detect *O*-GlcNAcylated proteins (Fig. 5O). We found 926 proteins from the SNc-VTA region and 919 proteins from the striatum (Supplementary Table 2), many of which were linked to the pathways relevant to neuronal and synaptic structure and function, including dopamine receptor-mediated signalling (Fig. 5P and Supplementary Tables 3 and 4). In this list, we confirmed the presence of previously known *O*-GlcNAcylated proteins such as bassoon, synapsin-1, ankyrin-G, and synaptopodin (Zachara and Hart, 2004; Vosseller *et al.*, 2006). We further identified potentially *O*-GlcNAcylated proteins, among which were glutamate receptors, GABA receptors, postsynaptic density (PSD) proteins, synaptic adhesion molecules, and neurotransmitter transporters. Importantly, TH and DAT, which are expressed by most midbrain dopamine neurons, were also found to be potentially *O*-GlcNAcylated (Supplementary Table 2). Thus, these results support the idea that *O*-GlcNAc modification may be essential for the proper structure and function of
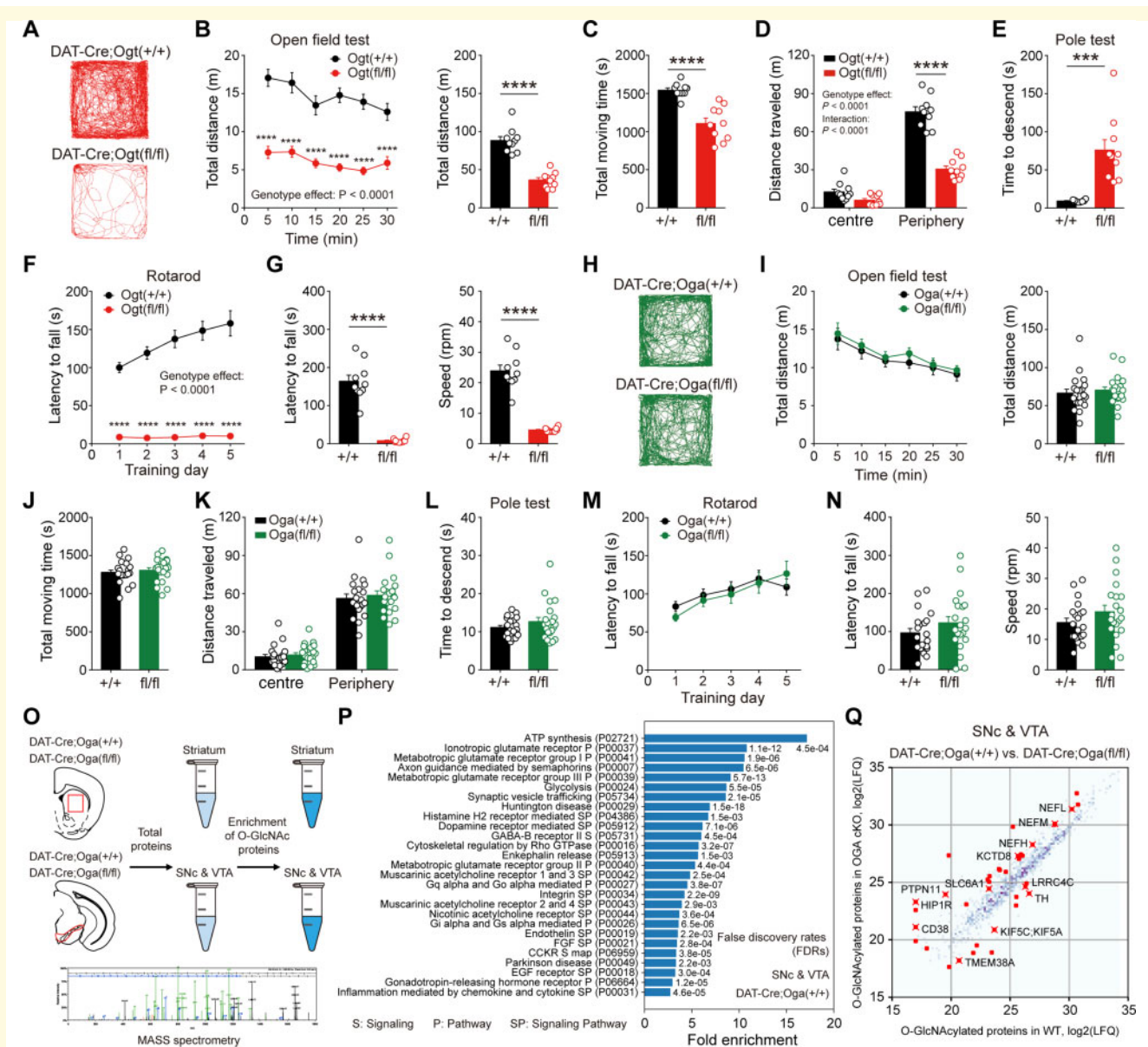
Figure 5 Manipulation of *O*-GlcNAcylation alters motor functions and the abundance of *O*-GlcNAcylated proteins. (A) Examples of movement path in the open field test in DAT-Cre;*Ogt*^{+/+} and DAT-Cre;*Ogt*^{fl/fl} mice. (**B** and **C**) Locomotive behaviour by total distance travelled and total moving time. (**D**) Thigmotaxis behaviour in the open field test. (**E**) Motor coordination in the pole test. (**F** and **G**) Motor learning and coordination in the rotarod test during training days and test days. (**H**) Examples of movement path in the open field test in DAT-Cre;*Oga*^{+/+} and DAT-Cre;*Oga*^{fl/fl} mice. (**I** and **J**) Locomotive behaviour by total distance travelled and total moving time. (**K**) Thigmotaxis behaviour in the open field test. (**L**) Motor coordination in the pole test. (**M** and **N**) Motor learning in the rotarod test during training days and test days. (**O**) Schematic illustration describing the sample preparation and mass spectrometry. (**P**) Pathways enriched in the identified proteins from SNc-VTA region with *O*-GlcNAcylation enrichment [>2-fold enrichment with the false discovery rate (FDR) <0.005]. (**Q**) Correlation of *O*-GlcNAcylation enriched protein abundance (LFQ intensity). We marked differentially abundant proteins between DAT-Cre;*Oga*^{+/+} and DAT-Cre;*Oga*^{fl/fl} mice with a red colour (<0.5- or >2-fold changes with FDR <0.05). Data were analysed by repeated measures two-way ANOVA followed by Sidak's *post hoc* test (**B, D, F, I, K** and **M**) and unpaired *t*-test (**B, C, E, G, I, J, L** and **N**). Data are represented as mean ± SEM. ***$P < 0.001$, ****$P < 0.0001$. WT = wild-type.

dopamine neurons. We next compared the abundance of *O*-GlcNAcylated proteins between wild-type and DAT-Cre;*Oga*^{fl/fl} mice in the midbrain SNc-VTA region, where dopamine neurons are predominantly located. In *Oga* cKO mice, we observed that the abundance of 37 proteins was significantly different compared to wild-types. It is

noteworthy that not all the *O*-GlcNAcylated proteins were more abundant in DAT-Cre;*Oga*^{fl/fl} mice (Fig. 5Q and Supplementary Table 5). Most interestingly, the abundance of *O*-GlcNAcylated TH was downregulated, suggesting that the direction of *O*-GlcNAc change can vary depending on specific proteins in DAT-Cre;*Oga*^{fl/fl} mice.

α-Synuclein-induced neurodegeneration is alleviated by genetic upregulation of O-GlcNAcylation

Studies consistently demonstrate that promoting *O*-GlcNAcylation protects against a wide range of cellular stresses. In the brain, *O*-GlcNAc modification, through cross-talk or interplay with phosphorylation, is significantly related to neurodegenerative diseases (Hart *et al.*, 2011; Wani *et al.*, 2017). Most proteins involved in Alzheimer's disease are *O*-GlcNAcylated (Wells *et al.*, 2001; Zachara and Hart, 2004). In addition, reduced *O*-GlcNAcylation is linked to the aetiology of Alzheimer's disease and increasing *O*-GlcNAcylation seems to mitigate pathological manifestations of Alzheimer's disease via *O*-GlcNAc modification of microtubule-associated protein tau and γ-secretase that produces amyloid-β (Yuzwa *et al.*, 2012; Kim *et al.*, 2013). Despite these findings, the potential role of *O*-GlcNAcylation on Parkinson's disease pathology remains largely unknown and has not been directly demonstrated in Parkinson's disease animal models *in vivo*.

To test whether the upregulation of *O*-GlcNAc can alleviate Parkinson's disease pathology *in vivo*, we injected AAVs expressing either wild-type α-synuclein or mutant form (A53T) unilaterally into the SNc area of DAT-Cre;*Oga*^{+/+} and DAT-Cre;*Oga*^{fl/fl} mice (Fig. 6A). These AAVs usually produce Parkinson's disease-like pathology at least 1–2 months after injection. Five weeks after virus injection, α-synuclein A53T virus induced pronounced Parkinson's disease pathology in SNc and DLS of ipsilateral hemisphere in DAT-Cre;*Oga*^{+/+} mice. The number of TH-positive dopamine neurons, TH-positive area, and TH intensity were remarkably decreased in the SNc of ipsilateral side when compared with the contralateral hemisphere (Fig. 6B–D). DAT-Cre;*Oga*^{+/+} mice also showed the degeneration of TH- and DAT-positive axonal processes along with reduced TH and DAT intensities in DLS (Fig. 6F–H), suggesting that A53T virus led to the degeneration of dopamine neurons and axons in wild-type littermate mice. Most remarkably, however, DAT-Cre;*Oga*^{fl/fl} mice exhibited much weaker Parkinson's disease-like pathology in the SNc and DLS of the ipsilateral hemisphere. Dopamine neurons in the SNc as well as axon fibres in the DLS only marginally degenerated 5 weeks after A53T virus injection (Fig. 6B–H). Moreover, the percentage of α-synuclein-positive dopamine neurons in the SNc of the ipsilateral side were significantly lower in DAT-Cre;*Oga*^{fl/fl} mice than the one in wild-types (Fig. 6E). We then analysed the number of presynaptic puncta with strong α-synuclein signal that might represent the aggregation of α-synuclein at synaptic boutons. In wild-type littermates, α-synuclein signal was significantly elevated in the ipsilateral side of the DLS, whereas smaller numbers of α-synuclein-positive boutons were observed in DAT-Cre;*Oga*^{fl/fl} mice (Fig. 6I). We further checked the levels of phosphorylated α-synuclein at S129 (pS129) in DLS, which

are highly related to α-synuclein pathology in Parkinson's disease (Anderson *et al.*, 2006; Oueslati, 2016) and found that the percentage of co-localization between α-synuclein and pS129 was significantly higher in DAT-Cre;*Oga*^{+/+} mice than in DAT-Cre;*Oga*^{fl/fl} mice (Fig. 6J and K). A53T virus infused in SNc spread into the neighbouring region and infected neurons in the VTA. Although much milder, upregulation of *O*-GlcNAc in DAT-Cre;*Oga*^{fl/fl} mice also exerted slightly protective effects on Parkinson's disease-like pathology in the VTA and NAc (Supplementary Fig. 6). Degeneration of dopamine neurons by wild-type α-synuclein was very moderate in DAT-Cre;*Oga*^{+/+} mice, but the protective effect from Parkinson's disease-like pathology by upregulated *O*-GlcNAc was again evident in DAT-Cre;*Oga*^{fl/fl} mice (Supplementary Fig. 7). Thus, our data possibly support the idea that upregulation of *O*-GlcNAcylation *in vivo* may make dopamine neurons less susceptible to pathological insults by Parkinson's disease via blocking the aggregation of α-synuclein.

Elevated O-GlcNAcylation mitigates impairments in dopamine transmission and motor learning caused by α-synuclein

To further determine the physiological significance of this protection against Parkinson's disease-like pathology, we measured the release of dopamine at dopamine synapses from the mice injected with A53T α-synuclein virus (Fig. 7A). Dopamine release by optogenetic stimulation was dramatically diminished in the DLS of the ipsilateral hemisphere in DAT-Cre;Ai32;*Oga*^{+/+} mice (Fig. 7B and C). Consistent with our immunostaining data, the release of dopamine, although reduced by A53T viral injection, was less compromised in the DLS of the ipsilateral hemisphere in DAT-Cre;Ai32;*Oga*^{fl/fl} mice (Fig. 7B and C). Importantly, the extent of dopamine release in the ipsilateral side of DAT-Cre;Ai32;*Oga*^{fl/fl} mice appeared to be comparable to the one in contralateral side of wild-type littermates, demonstrating that increased *O*-GlcNAcylation exerts a protective effect against functional deterioration following α-synuclein viral injection.

Lastly, we investigated whether the upregulated *O*-GlcNAcylation can be protective of motor deficits caused by α-synuclein expression in dopamine neurons. We injected either PBS or α-synuclein (A53T) AAV virus unilaterally into SNc in DAT-Cre;*Oga*^{+/+} and DAT-Cre;*Oga*^{fl/fl} mice. In the open field test, the viral expression of mutant α-synuclein did not result in any impairments of ambulatory locomotion irrespective of the genotypes. No changes were observed in both total distance and time travelled in the open field among the groups, showing that 5 weeks incubation after α-synuclein viral injection is insufficient to cause locomotor deficit (Fig. 7D–F). Comparable findings were also obtained from the cylinder test in which unilateral nigrostriatal damage generally causes the preferential use of the forelimb ipsilateral paw (the paw in the same side of the
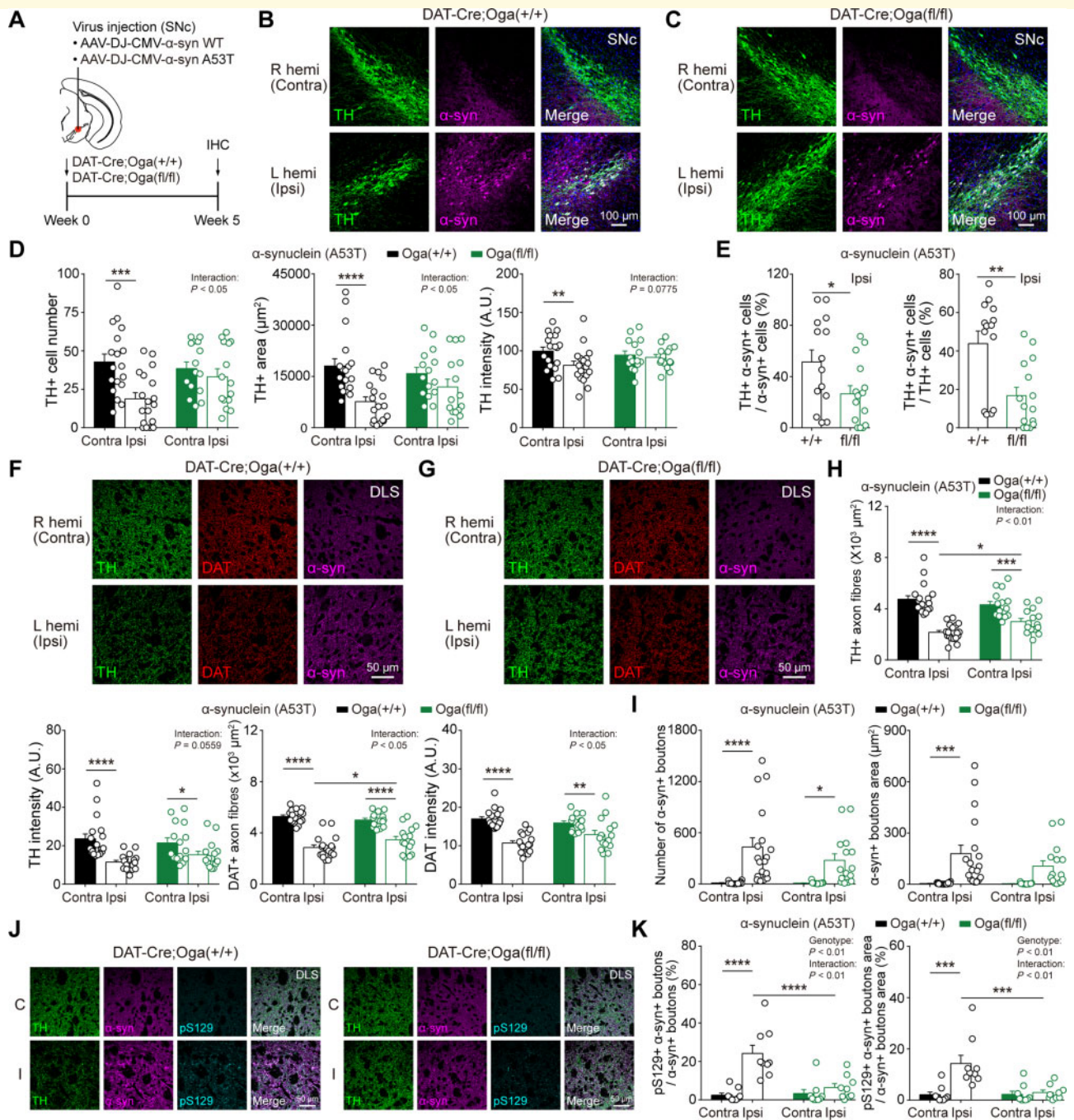
Figure 6 α-Synuclein-induced neurodegeneration is alleviated by upregulation of O-GlcNAcylation. (**A**) Schematic illustration describing the injection of α-synuclein AAV viruses [wild-type (WT) and A53T] into SNc (left hemisphere). (**B** and **C**) Representative confocal images of TH and α-synuclein immunofluorescence from SNc dopamine neurons in DAT-Cre;*Oga*$^{+/+}$ and DAT-Cre;*Oga*$^{fl/fl}$ mice injected with A53T virus. (**D**) Quantification and summary statistics of TH immunoreactivity in SNc. (**E**) Co-localization of TH and α-synuclein in ipsilateral SNc. (**F** and **G**) Representative confocal images of TH, DAT, and α-synuclein immunofluorescence from DLS in DAT-Cre;*Oga*$^{+/+}$ and DAT-Cre;*Oga*$^{fl/fl}$ mice injected with A53T virus. (**H**) Summary statistics of TH and DAT immunoreactivities in DLS. (**I**) The number and area of putative α-synuclein + synaptic boutons in DLS. (**J**) Representative confocal images of TH, α-synuclein, and pS129 immunofluorescence from DLS in DAT-Cre;*Oga*$^{+/+}$ and DAT-Cre;*Oga*$^{fl/fl}$ mice injected with A53T virus. C = contralateral; I = ipsilateral. (**K**) Co-localization of α-synuclein and pS129 in DLS. Data were analysed by repeated measures two-way ANOVA followed by Sidak's *post hoc* test (**D**, **H**, **I** and **K**) and unpaired *t*-test (**E**). Data are represented as mean ± SEM. *$P < 0.05$, **$P < 0.01$, ***$P < 0.001$, ****$P < 0.0001$.

damage) in mice. As with the locomotion in the open field, DAT-Cre;*Oga*^fl/fl mice as well as DAT-Cre;*Oga*^+/+ mice exhibited intact rearing behaviour in a transparent cylinder after α-synuclein injection (Fig. 7G). However, contralateral forelimb contacts were significantly lowered in DAT-Cre;*Oga*^+/+ mice injected with α-synuclein virus, while this preferential use of ipsilateral paw was only marginal in α-synuclein virus-injected DAT-Cre;*Oga*^fl/fl mice (Fig. 7H). Motor dysfunction by α-synuclein expression was also validated with the wire-hanging test. DAT-Cre;*Oga*^+/+ mice injected with α-synuclein virus quickly fell to the floor in the wire-hanging test compared with other groups (Fig. 7I). Remarkably, however, hanging performance was intact in DAT-Cre;*Oga*^fl/fl mice infused with α-synuclein virus. They hanged longer on the wire and fell less often than virus-injected DAT-Cre;*Oga*^+/+ mice (Fig. 7I). Most importantly, DAT-Cre;*Oga*^+/+ mice injected with α-synuclein virus failed to establish motor learning and

motor coordination in the rotarod test. Yet, α-synuclein virus-injected DAT-Cre;*Oga*^fl/fl mice were normally able to learn to coordinate limb movement and postural adjustment over the training days, leading to the acquisition of motor learning (Fig. 7J and K). These data strongly support the conclusion that the upregulation of *O*-GlcNAc modification in dopamine neurons alleviates and normalizes behavioural deficits in a mouse model of Parkinson's disease.

Pharmacological upregulation of *O*-GlcNAcylation also relieves α-synuclein-induced neurodegeneration and pathology

To explore the potential protection of dopamine neurons by pharmacological upregulation of *O*-GlcNAcylation, we first injected AAV α-synuclein virus (A53T) unilaterally into the
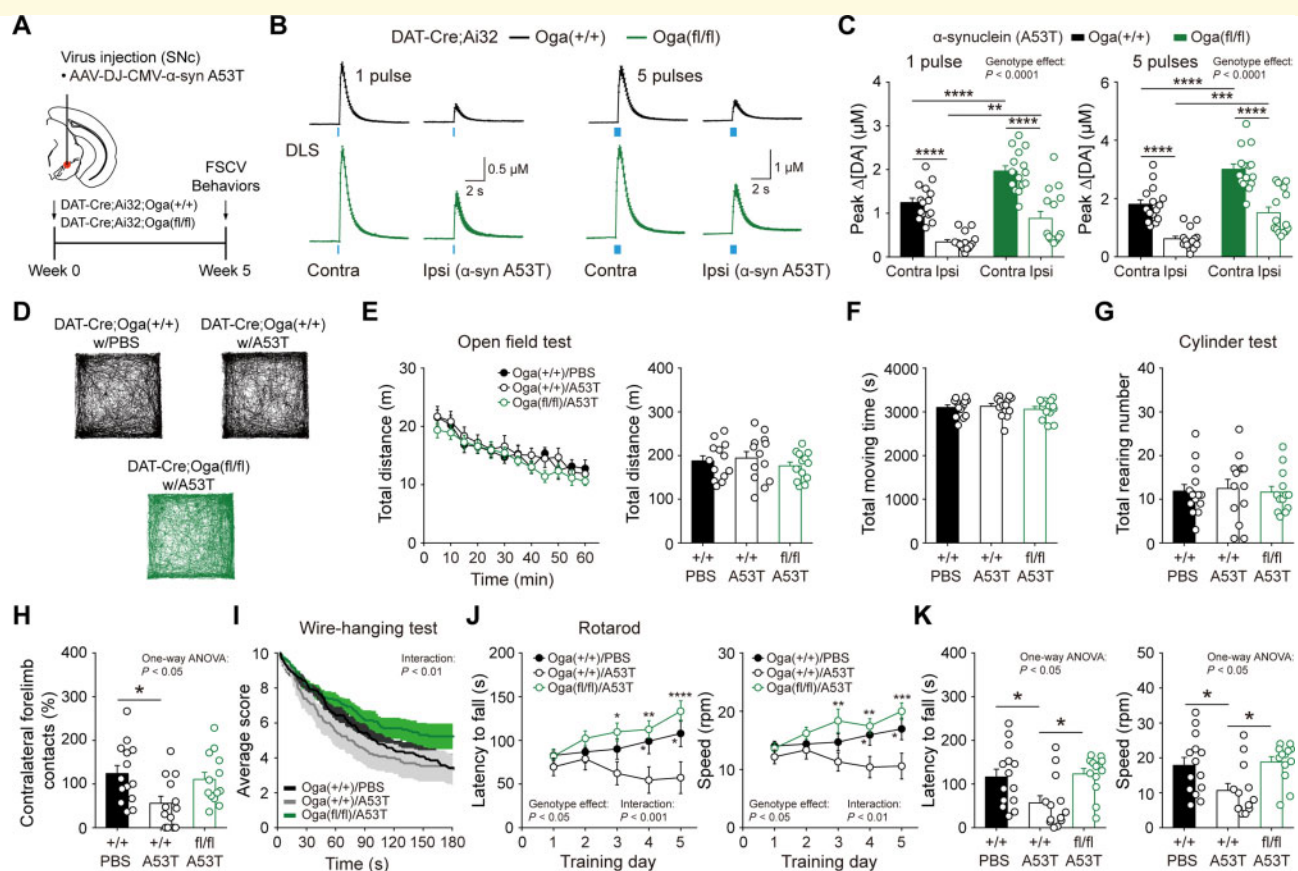

Figure 7 Elevated *O*-GlcNAcylation mitigates impairments in dopamine transmission and motor learning caused by α-synuclein. (**A**) Schematic illustration depicting the injection of α-synuclein AAV virus (A53T) into SNc (left hemisphere). (**B** and **C**) Quantification and summary statistics of dopamine release evoked by one pulse or five pulse stimulation in DLS from DAT-Cre;Ai32;*Oga*^+/+ and DAT-Cre;Ai32;*Oga*^fl/fl mice injected with α-synuclein (A53T) virus. (**D**) Examples of movement path in the open field test in DAT-Cre;*Oga*^+/+ and DAT-Cre;*Oga*^fl/fl mice injected with either PBS or α-synuclein (A53T) virus. (**E** and **F**) Locomotive behaviour by total distance travelled and total moving time in the open field test. (**G** and **H**) Summary statistics for rearing behaviour in the cylinder test. (**I**) Performances in the wire-hanging test. (**J** and **K**) Motor learning in the rotarod test during training days and test days. Blue bar indicates 450 nm light stimulation. Data were analysed by repeated measures two-way ANOVA followed by Sidak's *post hoc* test (**C**, **E**, **I** and **J**) and one-way ANOVA followed by Sidak's *post hoc* test (**E–H** and **K**). Data are represented as mean ± SEM. *$P < 0.05$, **$P < 0.01$, ***$P < 0.001$, ****$P < 0.0001$.

SNc area of DAT-Cre mice. Then, we injected the selective OGA inhibitor (thiamet G) daily at 3 weeks after virus injection for 2 weeks to temporarily elevate the level of *O*-GlcNAcylation (Fig. 8A). We found that *O*-GlcNAcylation was universally upregulated in the SNc area by 2 weeks injection of Thiamet G (Fig. 8B and C). Moreover, consistent with our findings in DAT-Cre;*Oga*fl/fl mice, pharmacological upregulation of *O*-GlcNAc also protected dopamine neurons from degeneration by α-synuclein (Fig. 8D) and attenuated the accumulation of pathological pS129 α-synuclein in the SNc (Fig. 8E and F). We further examined TH-positive axon fibres and pS129-positive synaptic boutons in the DLS and validated that pharmacological elevation of *O*-GlcNAcylation by OGA inhibition significantly alleviated the degeneration of TH-positive axons (Fig. 8G–J). In addition, the immunoreactivity of pS129 α-synuclein was reduced by Thiamet G injection (Fig. 8K and L). Taken together, pharmacological elevation of *O*-GlcNAc can be also effective in preventing and ameliorating Parkinson's disease-related pathology.

Discussion

Dopamine neurons in the midbrain and their axons in multiple brain regions, both of which constitute the midbrain dopamine system, function to govern and coordinate a plethora of motor and cognitive processes. Although functionally important, this midbrain dopamine system is prone to degeneration in neurological disorders, especially in Parkinson's disease because of its cellular and physiological properties (Lotharius and Brundin, 2002; Moore *et al.*, 2005; Roselli and Caroni, 2015). Therefore, it is imperative to develop diverse therapeutic strategies to protect the dopamine system against pathological insults from Parkinson's disease. Here, we identified the *O*-GlcNAcylation as a critical protein modification for regulating physiological function, survival, and degeneration of dopamine neurons in health and Parkinson's disease. The physiological roles of *O*-GlcNAcylation in the brain are gradually emerging owing to advances made in the field and a variety of neuronal proteins are being reported to be *O*-GlcNAcylated. Because of the lack of cell type-selective studies, however, a definitive functional role of *O*-GlcNAcylation in specific neuronal systems is still yet to be uncovered. Midbrain dopamine neurons are critical for voluntary movement, action selection, and reward-based learning (Schultz, 2007; Engelhard *et al.*, 2019), while structural and functional abnormalities in dopamine neurons cause numerous psychiatric and neurological disorders (Chuhma *et al.*, 2017; Surmeier *et al.*, 2017). Previous studies about neuronal *O*-GlcNAcylation have focused on its potential role in nutrient sensing, energy intake, and metabolism (Ruan *et al.*, 2014; Lagerlof *et al.*, 2016; Dai *et al.*, 2018). We found that selective downregulation of *O*-GlcNAc level in dopamine neurons lead to early synapse loss, degeneration, and functional deficits, eventually causing severe motor dysfunctions and premature mortality.

DAT-Cre;*Ogt*fl/fl mice grow and behave normally at 3 weeks of age. However, significantly lower body weight and serious impairment in motor functions are observed in adulthood. Although the downregulation of *O*-GlcNAcylation in dopamine neurons caused synaptic loss in both the DLS and NAc of 3-week-old DAT-Cre;*Ogt*fl/fl mice, the number of dopamine neurons in the midbrain was only marginally affected. Given both the postmitotic expression of DAT (Prakash and Wurst, 2006; Abeliovich and Hammond, 2007) and the limited effect of *O*-GlcNAc downregulation on dopamine cell number at 3 weeks of age, it is conceivable that *O*-GlcNAcylation in dopamine neurons is critical for the outgrowth, maintenance, and survival of dopaminergic neurites at young age, while the decreased *O*-GlcNAcylation could contribute to premature functional impairment and progressive degeneration of dopamine neurons with an age-dependent manner.

Elevated *O*-GlcNAcylation by the genetic deletion of *Oga*, on the other hand, enhances dopaminergic functions, without producing any detrimental effects on dopamine neuron structure and dopamine-mediated behaviours. No structural abnormalities, including dendrites, axonal arborizations, and dopamine cell number were found by the upregulation of *O*-GlcNAcylation. In addition, dopamine-modulated motor and cognitive functions are intact in DAT-Cre;*Oga*fl/fl mice. These results are surprising and in contrast to the recent finding where pan-neuronal upregulation of *O*-GlcNAcylation resulted in marked anatomical brain abnormalities, growth defects, and dysregulated metabolism (Olivier-Van Stichelen *et al.*, 2017). Most notably, synaptic transmission at dopamine terminals is remarkably facilitated by *O*-GlcNAc upregulation. Elevated *O*-GlcNAcylation led to selective increase in the amplitude of miniature excitatory transmission to dopamine neurons without any change in mEPSC frequency, possibly indicating that AMPA (α-amino-3-hydroxy-5-methyl-4-isoxazolepropionic acid) receptor function or its expression in dopamine neurons may be regulated by elevated *O*-GlcNAc modification (Kanno *et al.*, 2010; Taylor *et al.*, 2014).

At dopamine terminals in the DLS and NAc, dopamine transmission to spiny projection neurons is significantly enhanced by the upregulation of *O*-GlcNAcylation. In the brain, cytosolic *O*-GlcNAcylation is abundant at synaptic terminals (Cole and Hart, 2001). Furthermore, numerous presynaptic proteins, such as synapsin-1, bassoon, and piccolo, which have been reported to modulate presynaptic function and neurotransmitter release, are *O*-GlcNAcylated (Cole and Hart, 1999; Vosseller *et al.*, 2006; Hwang and Rhim, 2018). Our proteomics data also support the previous findings, confirming the abundant *O*-GlcNAcylation of these proteins in the striatum. It is important to note that *O*-GlcNAcylation of presynaptic proteins, including synapsin-1, can regulate synaptic vesicle localization and the size of the synaptic vesicle pool (Skorobogatko *et al.*, 2014), plausibly functioning to promote synaptic transmission, as in our result. Nevertheless, the overall regulation of *O*-GlcNAcylation in specific neurons seems to be more
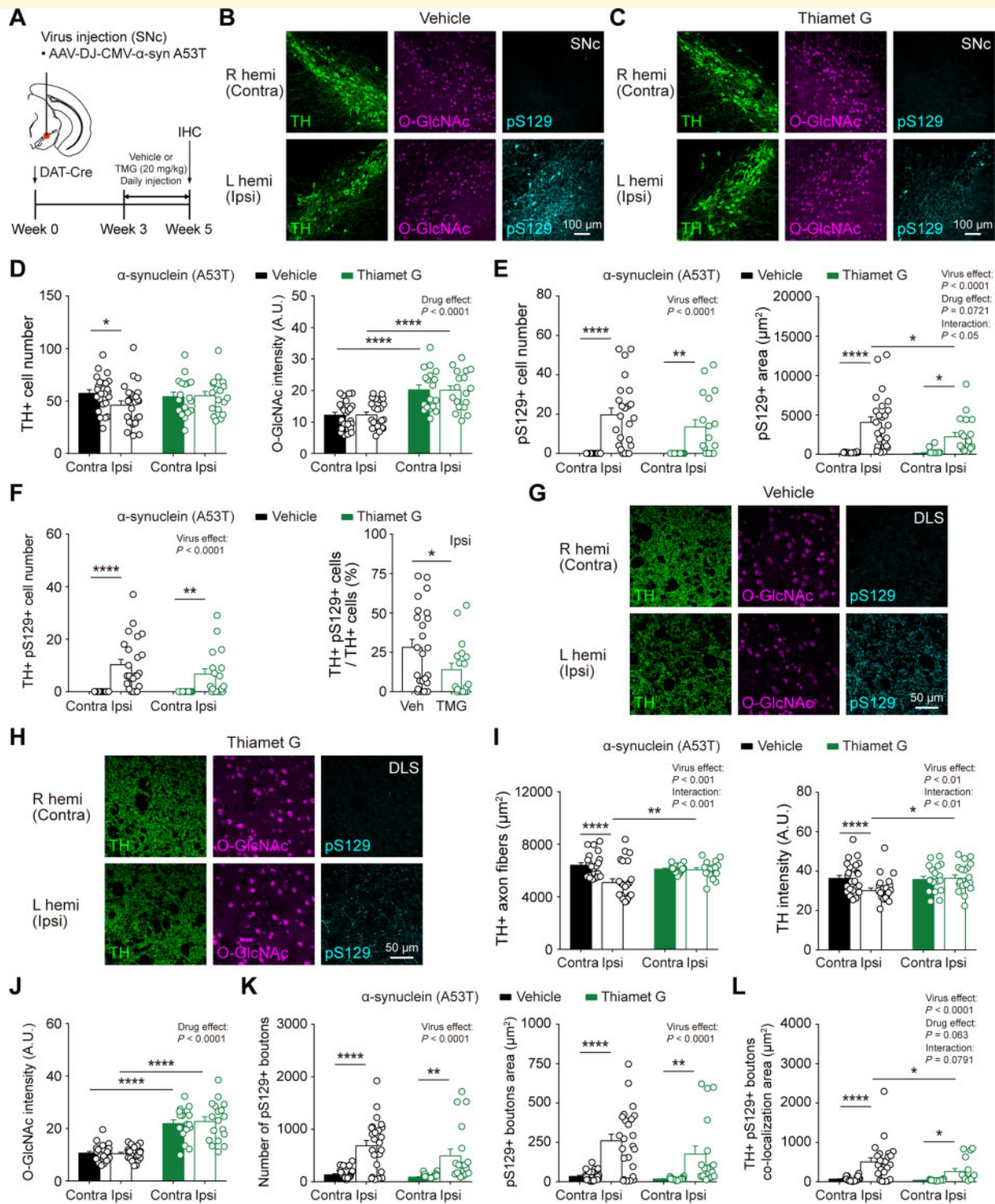
Figure 8 Pharmacological *O*-GlcNAc elevation also relieves the degeneration and pathology in dopamine neurons caused by α-synuclein expression. (**A**) Schematic illustration describing the injection of α-synuclein AAV virus (A53T) into SNc (left hemisphere) and intraperitoneal injection of Thiamet G (TMG) and vehicle. (**B** and **C**) Representative confocal images of TH, *O*-GlcNAc, and phospho-Ser129 α-synuclein (pS129) immunofluorescence from SNc in vehicle- and TMG-injected mice. (**D**) Quantification and summary statistics of TH and *O*-GlcNAc immunoreactivities in SNc. (**E**) Quantification and summary statistics of pS129 immunoreactivities in SNc. (**F**) Co-localization of TH and pS129 in SNc. (**G** and **H**) Representative confocal images of TH, *O*-GlcNAc, and pS129 immunofluorescence from DLS in vehicle- and TMG-injected mice. (**I**) Quantification and summary statistics of TH immunoreactivities in DLS. (**J**) Quantification and summary statistics of *O*-GlcNAc immunoreactivities in DLS. (**K**) Quantification and summary statistics of pS129 immunoreactivities in DLS. (**L**) Co-localization of TH and pS129 in DLS. Data were analysed by repeated measures two-way ANOVA followed by Sidak's *post hoc* test (**D–F** and **I–L**) and unpaired *t*-test (**F**). Data are represented as mean ± SEM. *P < 0.05, **P < 0.01, ****P < 0.0001.

complicated than we expect. When measured by immunostaining, overall *O*-GlcNAc intensities in dopamine neurons were increased by the genetic loss of *Oga*. However, the genetic deletion of *Oga* did not lead to the upregulation of *O*-GlcNAcylation in TH, but rather downregulated the abundance of *O*-GlcNAcylated TH. Given that neither TH-positive cell number nor TH intensity were affected in the SNc-VTA area, it is thus likely that the loss of *Oga* in dopamine neurons causes the downregulation of *O*-GlcNAcylated TH. This attenuated *O*-GlcNAcylation might, in turn, dynamically cross talk with phosphorylation and modulate the function of TH and dopamine release (Dunkley *et al.*, 2004; Hart *et al.*, 2011; Dunkley and Dickson, 2019). Bringing these considerations together, our results point to a notion that *O*-GlcNAcylation can critically regulate dopamine transmission via synaptic vesicle- and dopamine-related proteins. Therefore, our studies clearly indicate that beyond its well-known role as a nutrient-driven mediator of cell signalling, *O*-GlcNAcylation may play a vital role in ubiquitously modulating structures and functions of the neuronal system. Future studies are also needed to dissect out the molecular mechanisms markedly affected in dopamine neurons by *O*-GlcNAcylation.

Neuronal *O*-GlcNAcylation undergoes an age-dependent decline in normal ageing (Liu *et al.*, 2012) and increased *O*-GlcNAc modification seems to rescue neural and behavioural dysfunctions accompanied by the ageing process (Wheatley *et al.*, 2019). *O*-GlcNAcylation is also highly associated with neurodegeneration (Wang *et al.*, 2016; Wani *et al.*, 2017) and the manipulation of *O*-GlcNAc level appears to protect against neurodegeneration in pathological ageing such as Alzheimer's disease (Yuzwa *et al.*, 2012; Kim *et al.*, 2013). Nevertheless, this protective effect is far from proven and remains to be intensively investigated *in vivo*. In Parkinson's disease, aggregated α-synuclein is a hallmark of the disease and importantly, α-synuclein is *O*-GlcNAc modified in the brain (Wang *et al.*, 2010a; Alfaro *et al.*, 2012). Interestingly, *O*-GlcNAc modification has been recently shown to reduce α-synuclein aggregation *in vitro* when tested with purified proteins (Marotta *et al.*, 2015; Levine *et al.*, 2019), while the therapeutic effect of *O*-GlcNAcylation on Parkinson's disease and decreasing α-synuclein toxicity has never been tested *in vivo*. Our data clearly suggest that upregulation of *O*-GlcNAcylation can be protective of Parkinson's disease pathology. Genetic elevation of *O*-GlcNAc selectively in dopamine neurons mitigated a progressive degeneration of dopamine terminals and neurons induced by A53T mutant α-synuclein. Moreover, pharmacological elevation of *O*-GlcNAc by inhibiting OGA significantly reduced the accumulation of pS129 α-synuclein caused by mutant α-synuclein expression. Upregulation of *O*-GlcNAcylation also alleviated the functional impairment in dopamine transmission stemming from Parkinson's disease pathology. At behavioural level, motor coordination, balance, and motor learning were not disrupted by the mutant α-synuclein expression, due to increased *O*-GlcNAcylation. These new findings strengthens the emerging notion that *O*-GlcNAcylation can beneficially promote cell survival from diverse cellular stress and protect neurons against aggregate-prone proteins by multiple mechanisms (Groves *et al.*, 2013; Yang and Qian, 2017). In our data, phosphorylation of α-synuclein at S129 was dramatically reduced by the upregulation of *O*-GlcNAcylation. Although much needs to be elucidated, *O*-GlcNAcylation may affect the phosphorylation of α-synuclein. Therefore, enhanced *O*-GlcNAc *in vivo* could make α-synuclein less prone to aggregation, which results in the attenuation of pathological aggregation of α-synuclein.

In addition, a subset of proteins found in our proteomics data, including huntingtin-interacting protein 1-related (HIP1R) and neurofilament-M (NEFM) (Fig. 5Q and Supplementary Table 5), are implicated in neuroprotection and *O*-GlcNAc status of these proteins might confer additional protection of dopamine neurons against degeneration (Deng *et al.*, 2008; Lauterbach *et al.*, 2012). Lastly, the activation of key proteins in dopamine neurons such as TH and DAT can be altered by the concomitant changes in *O*-GlcNAc modification, which might contribute to the enhanced functions and protection of dopamine neurons. Thus, our findings demonstrate that upregulation of *O*-GlcNAcylation *in vivo* can make dopamine neurons less susceptible to pathological insults by Parkinson's disease, possibly via blocking phosphorylation-mediated aggregation of α-synuclein and thereby promoting neuronal survival. It is important to note that the upregulation of *O*-GlcNAcylation in dopamine neurons does not cause any detrimental effects on cellular structures and physiological functions. Thus, elevating *O*-GlcNAcylation potentially by pharmacological means may prove therapeutically fruitful in the treatment of Parkinson's disease. Together, *O*-GlcNAcylation may serve as a potential target for intervention and upregulating brain *O*-GlcNAc might help mitigate Parkinson's disease pathology.

Acknowledgements

Funding

Competing interests

The authors report no competing interests.

Supplementary material

Supplementary material is available at *Brain* online.

References

Abeliovich A, Hammond R. Midbrain dopamine neuron differentiation: factors and fates. Dev Biol 2007; 304: 447–54.

Akan I, Olivier-Van Stichelen S, Bond MR, Hanover JA. Nutrient-driven O-GlcNAc in proteostasis and neurodegeneration. J Neurochem 2018; 144: 7–34.

Akimoto Y, Comer FI, Cole RN, Kudo A, Kawakami H, Hirano H, et al. Localization of the O-GlcNAc transferase and O-GlcNAc-modified proteins in rat cerebellar cortex. Brain Res 2003; 966: 194–205.

Alfaro JF, Gong CX, Monroe ME, Aldrich JT, Clauss TR, Purvine SO, et al. Tandem mass spectrometry identifies many mouse brain O-GlcNAcylated proteins including EGF domain-specific O-GlcNAc transferase targets. Proc Natl Acad Sci USA 2012; 109: 7280–5.

Anderson JP, Walker DE, Goldstein JM, de Laat R, Banducci K, Caccavello RJ, et al. Phosphorylation of Ser-129 is the dominant pathological modification of alpha-synuclein in familial and sporadic Lewy body disease. J Biol Chem 2006; 281: 29739–52.

Berke JD. What does dopamine mean? Nat Neurosci 2018; 21: 787–93.

Brichta L, Greengard P. Molecular determinants of selective dopaminergic vulnerability in Parkinson's disease: an update. Front Neuroanat 2014; 8: 152.

Chuhma N, Mingote S, Kalmbach A, Yetnikoff L, Rayport S. Heterogeneity in dopamine neuron synaptic actions across the striatum and its relevance for schizophrenia. Biol Psychiatry 2017; 81: 43–51.

Cole RN, Hart GW. Glycosylation sites flank phosphorylation sites on synapsin I: o -linked N-acetylglucosamine residues are localized within domains mediating synapsin I interactions. J Neurochem 1999; 73: 418–28.

Cole RN, Hart GW. Cytosolic O-glycosylation is abundant in nerve terminals. J Neurochem 2001; 79: 1080–9.

Dai CL, Gu JH, Liu F, Iqbal K, Gong CX. Neuronal O-GlcNAc transferase regulates appetite, body weight, and peripheral insulin resistance. Neurobiol Aging 2018; 70: 40–50.

Deng Y, Li B, Liu F, Iqbal K, Grundke-Iqbal I, Brandt R, et al. Regulation between O-GlcNAcylation and phosphorylation of neurofilament-M and their dysregulation in Alzheimer disease. FASEB J 2008; 22: 138–45.

Deng Y, Li B, Liu Y, Iqbal K, Grundke-Iqbal I, Gong CX. Dysregulation of insulin signaling, glucose transporters, O-GlcNAcylation, and phosphorylation of tau and neurofilaments in the brain: implication for Alzheimer's disease. Am J Pathol 2009; 175: 2089–98.

Dunkley PR, Bobrovskaya L, Graham ME, von Nagy-Felsobuki EI, Dickson PW. Tyrosine hydroxylase phosphorylation: regulation and consequences. J Neurochem 2004; 91: 1025–43.

Dunkley PR, Dickson PW. Tyrosine hydroxylase phosphorylation in vivo. J Neurochem 2019; 149: 706–28.

Engelhard B, Finkelstein J, Cox J, Fleming W, Jang HJ, Ornelas S, et al. Specialized coding of sensory, motor and cognitive variables in VTA dopamine neurons. Nature 2019; 570: 509–13.

Gerfen CR, Surmeier DJ. Modulation of striatal projection systems by dopamine. Annu Rev Neurosci 2011; 34: 441–66.

Groves JA, Lee A, Yildirir G, Zachara NE. Dynamic O-GlcNAcylation and its roles in the cellular stress response and homeostasis. Cell Stress Chaperones 2013; 18: 535–58.

Hart GW, Slawson C, Ramirez-Correa G, Lagerlof O. Cross talk between O-GlcNAcylation and phosphorylation: roles in signaling, transcription, and chronic disease. Annu Rev Biochem 2011; 80: 825–58.

Holt GD, Hart GW. The subcellular distribution of terminal N-acetylglucosamine moieties. Localization of a novel protein-saccharide linkage, O-linked GlcNAc. J Biol Chem 1986; 261: 8049–57.

Hwang H, Rhim H. Functional significance of O-GlcNAc modification in regulating neuronal properties. Pharmacol Res 2018; 129: 295–307.

Hwang H, Rhim H. Acutely elevated O-GlcNAcylation suppresses hippocampal activity by modulating both intrinsic and synaptic excitability factors. Sci Rep 2019; 9: 7287.

Kanno T, Yaguchi T, Nagata T, Mukasa T, Nishizaki T. Regulation of AMPA receptor trafficking by O-glycosylation. Neurochem Res 2010; 35: 782–8.

Keembiyehetty C, Love DC, Harwood KR, Gavrilova O, Comly ME, Hanover JA. Conditional knock-out reveals a requirement for O-linked N-Acetylglucosaminase (O-GlcNAcase) in metabolic homeostasis. J Biol Chem 2015; 290: 7097–113.

Khidekel N, Ficarro SB, Peters EC, Hsieh-Wilson LC. Exploring the O-GlcNAc proteome: direct identification of O-GlcNAc-modified proteins from the brain. Proc Natl Acad Sci USA 2004; 101: 13132–7.

Kim C, Nam DW, Park SY, Song H, Hong HS, Boo JH, et al. O-linked beta-N-acetylglucosaminidase inhibitor attenuates beta-amyloid plaque and rescues memory impairment. Neurobiol Aging 2013; 34: 275–85.

Kim JI, Ganesan S, Luo SX, Wu YW, Park E, Huang EJ, et al. Aldehyde dehydrogenase 1a1 mediates a GABA synthesis pathway in midbrain dopaminergic neurons. Science 2015; 350: 102–6.

Lagerlof O, Slocomb JE, Hong I, Aponte Y, Blackshaw S, Hart GW, et al. The nutrient sensor OGT in PVN neurons regulates feeding. Science 2016; 351: 1293–6.

Lauterbach EC, Fontenelle LF, Teixeira AL. The neuroprotective disease-modifying potential of psychotropics in Parkinson's disease. Parkinsons Dis 2012; 2012: 753548.

Levine PM, Galesic A, Balana AT, Mahul-Mellier AL, Navarro MX, De Leon CA, et al. alpha-Synuclein O-GlcNAcylation alters aggregation and toxicity, revealing certain residues as potential inhibitors of Parkinson's disease. Proc Natl Acad Sci USA 2019; 116: 1511–9.

Lisman JE, Grace AA. The hippocampal-VTA loop: controlling the entry of information into long-term memory. Neuron 2005; 46: 703–13.

Liu Y, Li X, Yu Y, Shi J, Liang Z, Run X, et al. Developmental regulation of protein O-GlcNAcylation, O-GlcNAc transferase, and O-GlcNAcase in mammalian brain. PLoS One 2012; 7: e43724.

Lotharius J, Brundin P. Pathogenesis of Parkinson's disease: dopamine, vesicles and alpha-synuclein. Nat Rev Neurosci 2002; 3: 932–42.

Love DC, Kochan J, Cathey RL, Shin SH, Hanover JA. Mitochondrial and nucleocytoplasmic targeting of O-linked GlcNAc transferase. J Cell Sci 2003; 116(Pt 4): 647–54.

Luo SX, Timbang L, Kim JI, Shang Y, Sandoval K, Tang AA, et al. TGF-beta signaling in dopaminergic neurons regulates dendritic growth, excitatory-inhibitory synaptic balance, and reversal learning. Cell Rep 2016; 17: 3233–45.

Marotta NP, Lin YH, Lewis YE, Ambroso MR, Zaro BW, Roth MT, et al. O-GlcNAc modification blocks the aggregation and toxicity of

the protein alpha-synuclein associated with Parkinson's disease. Nat Chem 2015; 7: 913–20.

Matsuda W, Furuta T, Nakamura KC, Hioki H, Fujiyama F, Arai R, et al. Single nigrostriatal dopaminergic neurons form widely spread and highly dense axonal arborizations in the neostriatum. J Neurosci 2009; 29: 444–53.

Moore DJ, West AB, Dawson VL, Dawson TM. Molecular pathophysiology of Parkinson's disease. Annu Rev Neurosci 2005; 28: 57–87.

Olivier-Van Stichelen S, Wang P, Comly M, Love DC, Hanover JA. Nutrient-driven O-linked N-acetylglucosamine (O-GlcNAc) cycling impacts neurodevelopmental timing and metabolism. J Biol Chem 2017; 292: 6076–85.

Oueslati A. Implication of alpha-synuclein phosphorylation at S129 in synucleinopathies: what have we learned in the last decade? J Parkinsons Dis 2016; 6: 39–51.

Prakash N, Wurst W. Development of dopaminergic neurons in the mammalian brain. Cell Mol Life Sci 2006; 63: 187–206.

Rex-Mathes M, Werner S, Strutas D, Griffith LS, Viebahn C, Thelen K, et al. O-GlcNAc expression in developing and ageing mouse brain. Biochimie 2001; 83: 583–90.

Roselli F, Caroni P. From intrinsic firing properties to selective neuronal vulnerability in neurodegenerative diseases. Neuron 2015; 85: 901–10.

Ruan HB, Dietrich MO, Liu ZW, Zimmer MR, Li MD, Singh JP, et al. O-GlcNAc transferase enables AgRP neurons to suppress browning of white fat. Cell 2014; 159: 306–17.

Schultz W. Multiple dopamine functions at different time courses. Annu Rev Neurosci 2007; 30: 259–88.

Skorobogatko Y, Landicho A, Chalkley RJ, Kossenkov AV, Gallo G, Vosseller K. O-linked beta-N-acetylglucosamine (O-GlcNAc) site thr-87 regulates synapsin I localization to synapses and size of the reserve pool of synaptic vesicles. J Biol Chem 2014; 289: 3602–12.

Surmeier DJ, Obeso JA, Halliday GM. Selective neuronal vulnerability in Parkinson disease. Nat Rev Neurosci 2017; 18: 101–13.

Taylor EW, Wang K, Nelson AR, Bredemann TM, Fraser KB, Clinton SM, et al. O-GlcNAcylation of AMPA receptor GluA2 is associated with a novel form of long-term depression at hippocampal synapses. J Neurosci 2014; 34: 10–21.

Tritsch NX, Ding JB, Sabatini BL. Dopaminergic neurons inhibit striatal output through non-canonical release of GABA. Nature 2012; 490: 262–6.

Vosseller K, Trinidad JC, Chalkley RJ, Specht CG, Thalhammer A, Lynn AJ, et al. O-linked N-acetylglucosamine proteomics of postsynaptic density preparations using lectin weak affinity chromatography and mass spectrometry. Mol Cell Proteomics 2006; 5: 923–34.

Wang AC, Jensen EH, Rexach JE, Vinters HV, Hsieh-Wilson LC. Loss of O-GlcNAc glycosylation in forebrain excitatory neurons induces neurodegeneration. Proc Natl Acad Sci USA 2016; 113: 15120–5.

Wang Z, Gucek M, Hart GW. Cross-talk between GlcNAcylation and phosphorylation: site-specific phosphorylation dynamics in response to globally elevated O-GlcNAc. Proc Natl Acad Sci USA 2008; 105: 13793–8.

Wang Z, Udeshi ND, O'Malley M, Shabanowitz J, Hunt DF, Hart GW. Enrichment and site mapping of O-linked N-acetylglucosamine by a combination of chemical/enzymatic tagging, photochemical cleavage, and electron transfer dissociation mass spectrometry. Mol Cell Proteomics 2010a; 9: 153–60.

Wang Z, Udeshi ND, Slawson C, Compton PD, Sakabe K, Cheung WD, et al. Extensive crosstalk between O-GlcNAcylation and phosphorylation regulates cytokinesis. Sci Signal 2010b; 3: ra2.

Wani WY, Chatham JC, Darley-Usmar V, McMahon LL, Zhang J. O-GlcNAcylation and neurodegeneration. Brain Res Bull 2017; 133: 80–7.

Watabe-Uchida M, Zhu L, Ogawa SK, Vamanrao A, Uchida N. Whole-brain mapping of direct inputs to midbrain dopamine neurons. Neuron 2012; 74: 858–73.

Wells L, Vosseller K, Hart GW. Glycosylation of nucleocytoplasmic proteins: signal transduction and O-GlcNAc. Science 2001; 291: 2376–8.

Wheatley EG, Albarran E, White CW, 3rd Bieri G, Sanchez-Diaz C, Pratt K, et al. Neuronal O-GlcNacylation improves cognitive function in the aged mouse brain. Curr Biol 2019; 29: 3359–69 e4.

Yang X, Qian K. Protein O-GlcNAcylation: emerging mechanisms and functions. Nat Rev Mol Cell Biol 2017; 18: 452–65.

Yang YR, Song M, Lee H, Jeon Y, Choi EJ, Jang HJ, et al. O-GlcNAcase is essential for embryonic development and maintenance of genomic stability. Aging Cell 2012; 11: 439–48.

Yuzwa SA, Shan X, Macauley MS, Clark T, Skorobogatko Y, Vosseller K, et al. Increasing O-GlcNAc slows neurodegeneration and stabilizes tau against aggregation. Nat Chem Biol 2012; 8: 393–9.

Zachara NE, Hart GW. O-GlcNAc a sensor of cellular state: the role of nucleocytoplasmic glycosylation in modulating cellular function in response to nutrition and stress. Biochim Biophys Acta 2004; 1673: 13–28.

Zachara NE, Hart GW. Cell signaling, the essential role of O-GlcNAc!. Biochim Biophys Acta 2006; 1761: 599–617.